A theoretical investigation on the photochemical performance of hybrid dye-sensitized solar cells based on Keggin-type polyoxometalates

Maryam Fallah, Bahram Yadollahi, and Reza Omidyan*

Department of Chemistry, University of Isfahan, Isfahan 81746-73441, Iran.

Supporting Information

Table of contents		Page No.
Theoretical background	Electron excitation analysis of dyes	S1-S4
Table S1	Comparison of optimized geometry	S5
Figure S1	The optimized molecular structure of DTP and DTP/POM	S5
Figure S2	Molecular orbitals	S6
Table S2	Electronic transition states	S7
Figure S3	Natural transition orbitals	S8
Table S3	C_{hole} & C_{ele} map	S9
Figure S4	Heat maps	S10
Figure S5	The percentage of each fragment	S11
Figure S6	Absorption spectra	S12
References		S12

1.1 Theoretical background of electron excitation analysis of dyes

To assess the ICT capabilities of dyes, various ICT parameters were calculated, including the quantity of transferred charges (q_{CT}), the effective charge transfer distance (d_{CT}), and the *t* index, which evaluates the separation degree between ρ^+ (r) and ρ^- (r) based on the total densities of both ground and excited states. The charge transfer (CT) length in X/Y/Z can be measured by distance between centroid of hole and electron in corresponding directions:

$$\boldsymbol{D_x} = |X_{ele} - X_{hole}| \qquad \boldsymbol{D_y} = |Y_{ele} - Y_{hole}| \qquad \boldsymbol{D_z} = |Z_{ele} - Z_{hole}|$$

The total magnitude of CT length is referred to as *D* index:

$$\boldsymbol{D}\ \textbf{index} = |D| \equiv \sqrt{(D_x)^2 + (D_y)^2 + (D_z)^2} \tag{1}$$

t index is designed to measure separation degree of hole and electron in CT direction:

$$\boldsymbol{t}\ \textbf{index} = \boldsymbol{D}\ \textbf{index} - \boldsymbol{H}_{\mathrm{CT}} \tag{2}$$

$H\lambda$ measures average degree of spatial extension of hole and electron distribution in X/Y/Z direction, H_{CT} is that in CT direction. Δr index has been established to enhance the investigation

of excited electronic states within the context of Time-Dependent Density Functional Theory, that is derived from the charge centroids of the orbitals participating in the excitations and can be understood in terms of the distance between the hole and the electron. The Δ*r* can be articulated as follows:

$$\Delta r = \sum_{i,a} \Delta r_i^a \quad (3)$$

The term Δr_i^a represents the contribution of the orbital transition from state *i* to state *a* in relation to the Δ*r* index:

$$\Delta r_{i=}^{a} \frac{\left(k_i^a\right)^2}{\sum_{i,a}\left(k_i^a\right)^2} |\langle \varphi_a | r | \varphi_a \rangle - \langle \varphi_i | r | \varphi_i \rangle| \quad (4)$$

The index *i* and *a* run over all occupied and virtual MOs, respectively. φ is orbital wave function. It is important to note that when an electron excitation can be accurately depicted by a one pair of molecular orbital transitions, the r index and *D* index established within the framework of hole-electron analysis will, in principle, be completely equivalent.

$$\Delta r = |\langle \varphi_a | r | \varphi_a \rangle - \langle \varphi_i | r | \varphi_i \rangle| \equiv \left| \int r |\varphi_a(r)|^2 dr - \int r |\varphi_i(r)|^2 dr \right| \quad (5)$$

$$D \text{ index} = |D| = \left| \int r \rho^{eIe}(r) dr - \int r \rho^{hole}(r) dr \right| = \left| \int r |\varphi_a(r)|^2 dr - \int r |\varphi_i(r)|^2 dr \right| \quad (6)$$

To characterize overlapping extent of hole and electron, S_r index is defined as follows:

$$\boldsymbol{S_r}\textbf{ index} = \int \boldsymbol{S_r}\,(\mathbf{r})\,\mathbf{dr} \equiv \int \sqrt{\rho^{hole}(r)\rho^{ele}(r)}\, dr \quad (7)$$

The distributions of holes and electrons frequently exhibit numerous nodes or intricate fluctuations. To facilitate a visual analysis of these distributions, the C_{hole} and C_{ele} functions have been introduced. The characteristics of the C_{hole} and C_{ele} functions resemble those of the Gaussian function; they are exceptionally smooth and their values asymptotically approach zero as one moves away from the centroid of the hole or electron distribution.[1]

$$\boldsymbol{C_{ele}}\,(\mathbf{r}) = \boldsymbol{A}_{\mathbf{ele}}\ \mathbf{exp}\left[-\frac{(x - X_{eLe})^2}{2\sigma_{ele,x}^2} - \frac{(y - Y_{ele})^2}{2\sigma_{ele,y}^2} - \frac{(z - Z_{ele})^2}{2\sigma_{ele,z}^2} \right] \quad (8)$$

$$\boldsymbol{C_{hole}}\,(\mathbf{r}) = \boldsymbol{A}_{\mathbf{hole}}\ \mathbf{exp}\left[-\frac{(x - X_{hole})^2}{2\sigma_{hole,x}^2} - \frac{(y - Y_{hole})^2}{2\sigma_{hole,y}^2} - \frac{(z - Z_{hole})^2}{2\sigma_{hole,z}^2} \right] \quad (9)$$

Coulomb attractive negative value is known as exciton binding energy, which is a positive value. This term can be calculated via simple Coulomb formula:

$$E_C = \iint \frac{\rho^{hole}(r_1)\rho^{ele}(r_2)}{|r_1 - r_2|} dr_1 dr_2 \quad (10)$$

1.2. Theoretical background of efficiency of dye-sensitized solar cells

The power conversion efficiency (*PCE*) in dye-sensitized solar cells (DSSCs) can be articulated as follow:[2]

$$PCE = \frac{Jsc \times Voc \times FF}{Pin} \times 100\% \quad (11)$$

In this context, J_{SC} represents the short-circuit photocurrent density, V_{OC} denotes the open-circuit photovoltage, P_{in} indicates the intensity of the incident light, and *FF* refers to the fill factor of the photovoltaic cell. Enhancing J_{SC} and V_{OC} represents a viable strategy for increasing *PCE*. J_{sc} is a crucial parameter expressed in the following manner:[3]

$$J_{sc} = \int LHE_{(\lambda)} \varphi_{inject} \eta_{collect} d\lambda \quad (12)$$

Light harvesting efficiency (*LHE*), electron injection efficiency (φ_{inject}), and charge collection efficiency ($\eta_{collect}$) are interconnected factors that play a crucial role in the overall performance of the system. In the case of dye-sensitized solar cells (DSSCs), the electrode remains consistent; the only difference is the various sensitizers. Therefore, $\eta_{collect}$ can be regarded as a constant. While the LHE is governed by the oscillator strength (*f*) that corresponds to the maximum absorption wavelength (λ_{max}). This relationship can be expressed as follows:[4]

$$LHE = 1\text{-}10^{-f} \quad (13)$$

The efficiency of electron injection (φ_{inject}), is directly related to the free enthalpy (ΔG_{inj}), which corresponds to the transfer of electrons from the excited states of dyes to the conduction band (CB) of TiO_2. ΔG parameter establishes the rate of electron injection and can be regarded as the driving force for electron injection. The following equations can be used to describe it:[5]

$$\Delta G_{inj} = E_{OX}^{dye*} - E_{CB}^{TiO_2} \quad (14)$$

$$E_{OX}^{dye*} = E_{OX}^{dye} - \Delta E \quad (15)$$

E_{OX}^{dye*} represents the excited state oxidation potential, while E_{OX}^{dye} represents the ground state oxidation potential. According to the Koopman theorem,[6] the negative E_{HOMO}^{dye} is assessed as the oxidation potential corresponding to the ground state (E_{OX}^{dye}).

The $E_{CB}^{TiO_2}$ indicates the conduction band edge of TiO_2. Accurately determining this value poses challenges due to its significant sensitivity to operating conditions, particularly the pH of the solution. In the current investigation, we have employed a value of -4.0 eV which aligns with the experimental conditions, where the semiconductor interfaces with aqueous redox electrolytes

maintained at a constant pH of 7.0.[7] ΔE denotes the vertical excitation energy. Lower ΔG_{inj} and higher *LHE* result in light harvesting efficiency higher J_{sc}.[8] The regeneration process, denoted as φ_{regen}, can be scaled in proportion to the Gibbs free energy of regeneration (ΔG_{regen}) associated with the oxidized dye and the iodine/iodide electrolyte. The Gibbs free energy of regeneration can be analyzed using Equation (16).[9]

$$\Delta \boldsymbol{G}_{\text{regen}} = \boldsymbol{E}_{\textbf{redox}} - \boldsymbol{E}_{\textbf{dye}} \tag{16}$$

$$\Delta \boldsymbol{G}_{\text{cr}} = E^{TiO_2}_{CB} - E_{\text{dye}} \tag{17}$$

The open-circuit voltage, V_{oc}, as presented in equation (11), pertains to the transfer of electrons from the excited dye to the conduction band of the semiconductor. This relationship is defined by the subsequent equation.

$$\boldsymbol{V_{oc}} = E_{LUMO} - E^{TiO_2}_{CB} \tag{18}$$

Table S1. Comparison of optimized geometry (bond lengths) at B3LYP and PBE methods and X-ray distances (in Å) for $[PW_{12}O_{40}]^{3-}$

Selected bond	B3LYP/6-31G(d)/LANL2DZ	PBE/6-31G(d)/LANL2DZ	Exp.[a]
X- O_{tetra}	1.55	1.57	1.53
W- O_{tetra}	2.45	2.45	2.43
X-W	3.59	3.60	3.49
W-O_{ter}	1.71	1.73	1.69
W-O_{brid}	1.92	1.93	1.93

[a]The experimental values were adapted from ref.10

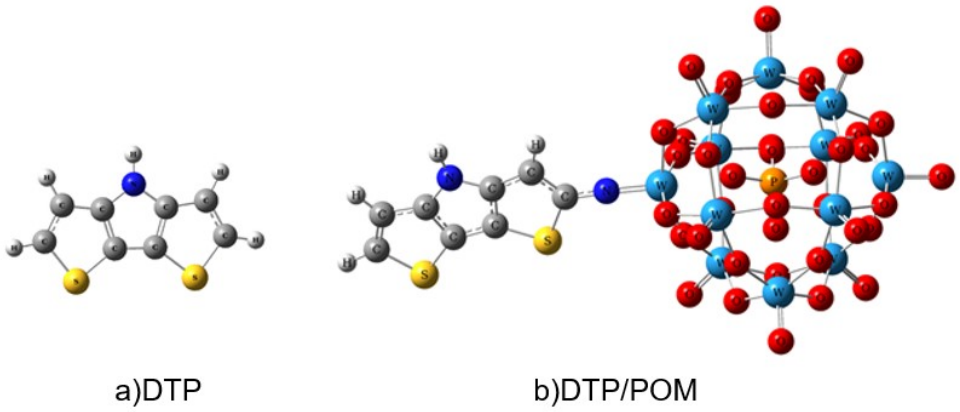

Figure S1. The optimized molecular structure of DTP and DTP/POM at B3LYP/6-31G(d)/LANL2DZ method

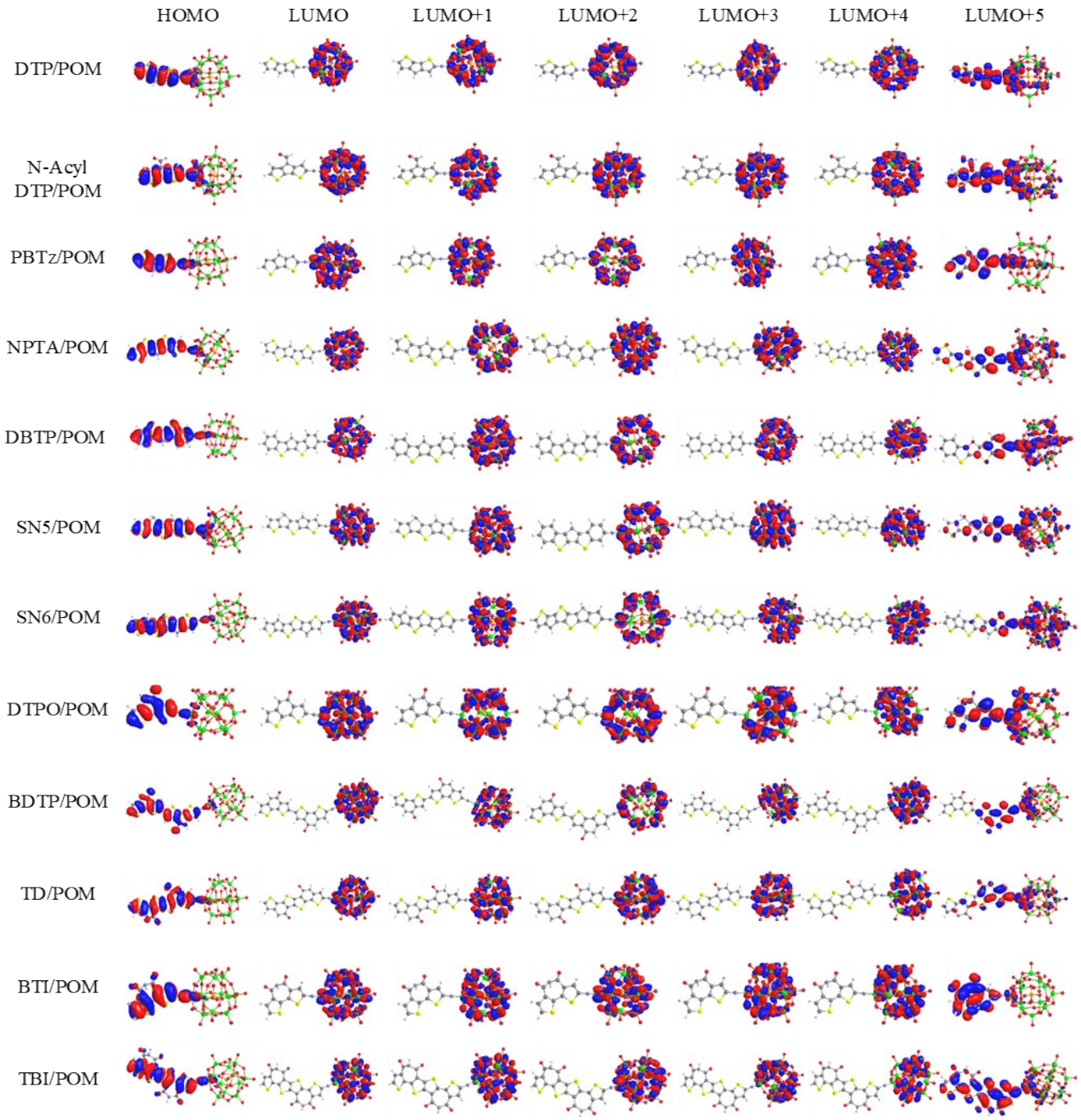

Figure S2. Molecular orbitals (MOs) for the studied designed hybrids

Table S2. Some electronic transition states, main transitions, and their contribution percentages, energy vertical, λ, and oscillator strengths of the studied designed hybrids (The electron transitions in the visible region with the highest oscillator strengths are bolded).

Dye	State	Transition	Contribution%	Energy (eV)	λ	*f*
DTP/POM	S3	H → L+5 H → L+2	34 29	2.86	433	0.6
	S4	**H → L+5** H → L+4 H → L+2	**52** 15 14	**2.88**	**431**	**0.9**
N-Acyl DTP/POM	**S3**	**H → L+5**	**87**	**2.68**	**421**	**1.46**
	S4	H→ L+2 H → L+4	20 20	3.07	403	0.016
PBTz/POM	**S3**	**H → L+5**	**88**	**2.92**	**424**	**1.37**
	S4	H → L+9	40	3.18	389	0.004
NPTA/POM	S2	H → L	70	2.4	518	0.01
	S3	**H → L+5**	**85**	**2.67**	**462**	**1.99**
	S4	H → L+4 H → L+2	42 42	2.8	442	0.007
DBTP/POM	**S3**	**H → L+4** H → L+5	**34** 28	**3.16**	**425**	**0.78**
	S4	H → L+5 H → L+4	44 23	3.19	390	1.28
SN5/POM	**S3**	**H → L+5** H → L+4	**72** 9	**2.55**	**480**	**1.78**
	S4	H → L+4 H → L+2	37 35	2.6	477	0.31
SN6/POM	**S3**	**H → L+5**	**81**	**2.55**	**486**	**2.31**
	S4	H → L+4 H → L+2	42 40	2.62	473	0.02
DTPO/POM	**S3**	**H → L+5**	**84.5**	**2.89**	**428**	**1.53**
	S4	H → L+4	24.5	3.1	388	0.003
BDTP/POM	**S2**	**H → L+5**	**77**	**2.61**	**474**	**2.07**
	S3	H → L H → L+1	44 35	2.67	463	0.029
TD/POM	**S2**	**H → L+5**	**74**	**2.67**	**464.5**	**1.82**
	S3	**H → L** H → L+1	**50** 27	**2.7**	**460**	**0.2**
BTI/POM	**S2**	**H → L+5**	**92**	**2.83**	**438**	**1.00**
	S3	H → L	79	3.1	399	0.00
TBI/POM	**S1**	**H → L+5**	**80**	**2.61**	**474**	**1.88**
	S2	H → L+1 H → L+4	37 12	2.63	470	0.07

NTO / Dye	Hole	Elec
DTP/POM	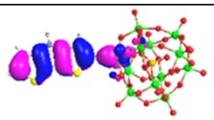	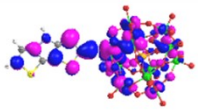
N-Acyl DTP/POM	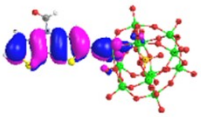	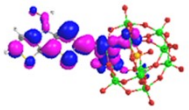
PBTz/POM	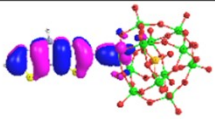	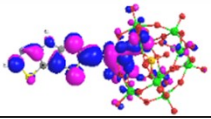
NPTA/POM	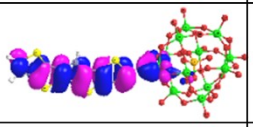	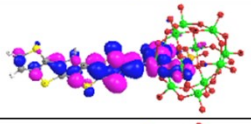
DBTP/POM	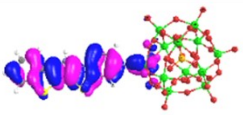	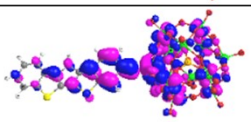
SN5/POM	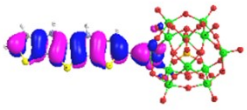	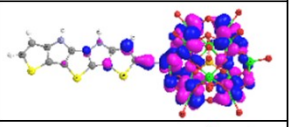
SN6/POM	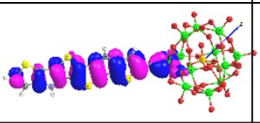	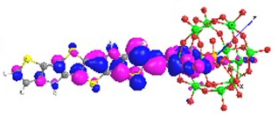
DTPO/POM	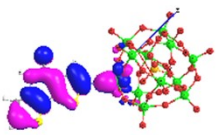	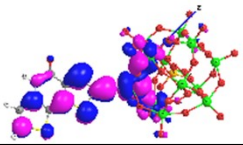
BDTP/POM	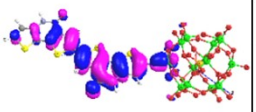	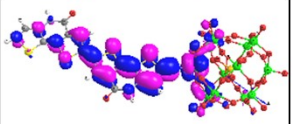
TD/POM	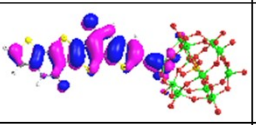	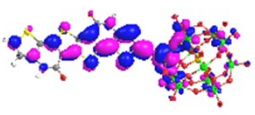
BTI/POM	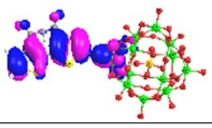	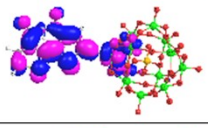
TBI/POM	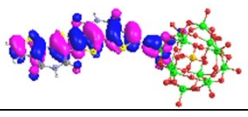	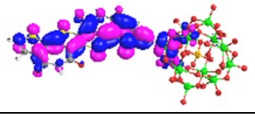

Figure S3. NTO_S of the studied designed hybrids

Table S3. CDD, C_{hole} & C_{ele} map, Δr, S_r and t index of the studied designed hybrids (Green and blue show hole and electron respectively)

Dye	CDD	C_{hole} & C_{ele} map	Δ r (Å)	S_r
N-Acyl DTP/POM	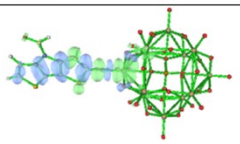	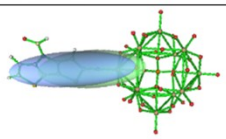	3.45	0.78
PBTz/POM	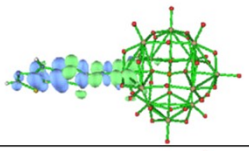	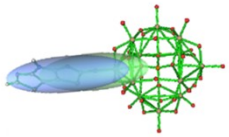	3.76	0.77
NPTA/POM	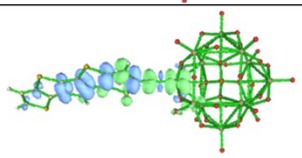	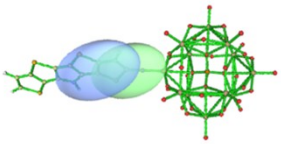	5.19	0.76
SN5/POM(S3)	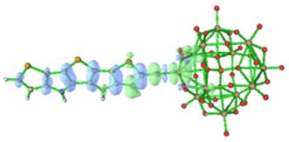	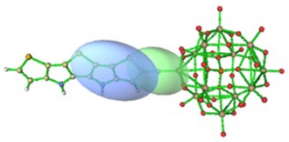	6.02	0.70
DTPO/POM	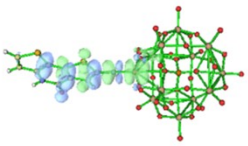	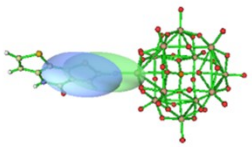	3.81	0.77
TD/POM(S2)	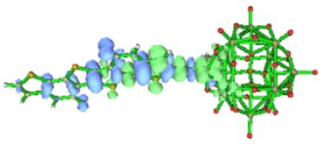	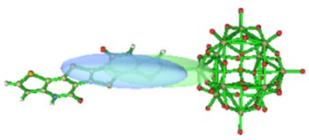	6.09	0.77
BTI/POM	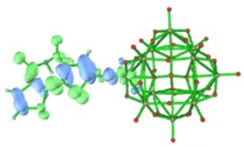	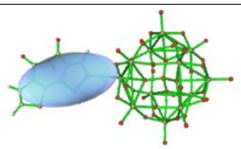	1.09	0.79
TBI/POM	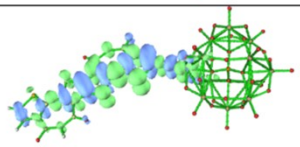	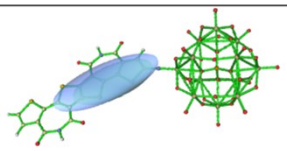	3.20	0.81

CDD = charge density difference

C_{hole} & C_{ele} map = graph of the distance between the center of the hole and the electron

D index = Hole–electron distance

S_r = overlap between the hole and the electron

t index = separation degree of hole and electron in CT direction.

DBTP/POM

DBTP **: Hole: 81.02 %** Electron: 18.57 %
N **:** Hole: 4.51 % Electron: 2.94 %
POM **:** Hole: 14.47 % **Electron: 78.48 %**

Transferred electrons between fragments:

1 → 2 0.02384	2 → 1 0.00837	Net 1→2 0.01547
1 → 3 0.63589	**3 → 1 0.02688**	**Net 1→ 3 0.60901**
2 →3 0.03537	3 → 2 0.00426	Net 2→ 3 0.03111

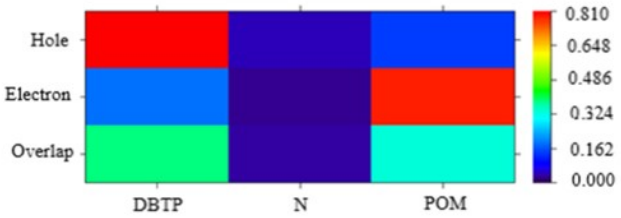

SN5/POM

SN5 **: Hole: 76.42 %** Electron: 6.99 %
N **:** Hole: 2.72 % Electron: 1.54 %
POM **:** Hole: 20.86 % **Electron: 91.47 %**

Transferred electrons between fragments:

1 → 2 0.01175	2 → 1 0.00190	Net 1 → 2 0.00985
1 → 3 0.69907	**3 → 1 0.01458**	**Net 1 → 3 0.68449**
2 → 3 0.02486	3 → 2 0.00321	Net 2 → 3 0.02165

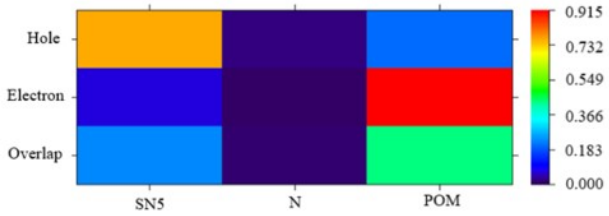

SN6/POM

SN6 : Hole: 80.82 % Electron: 50.75 %
N : Hole: 2.05 % Electron: 8.62 %
POM **:** Hole: 17.13 % Electron: 40.62 %

Transferred electrons between fragments:

1→ 2: 0.06969	2 →1: 0.01043	Net 1 → 2: 0.05926
1→ 3: 0.32829	**3 →1: 0.08694**	**Net 1 → 3: 0.24135**
2→ 3: 0.00835	3 → 2: 0.01477	Net 2 → 3: -0.00643

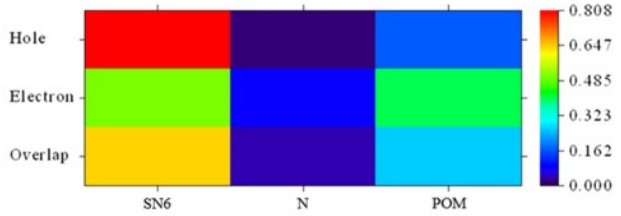

BDTP/POM

BDTP : Hole: 86.42 % Electron: 66.19 %
N : Holc: 2.76 % Electron: 3.66 %
POM : Hole: 10.81 % Electron: 30.16 %

Transferred electrons between fragments:

1 → 2: 0.03159	2 →1: 0.01827	Net 1 → 2: 0.01332
1 → 3: 0.26064	**3 →1: 0.07158**	**Net 1 →3: 0.18907**
2 → 3: 0.00833	3 →2: 0.00395	Net 2 → 3: 0.00437

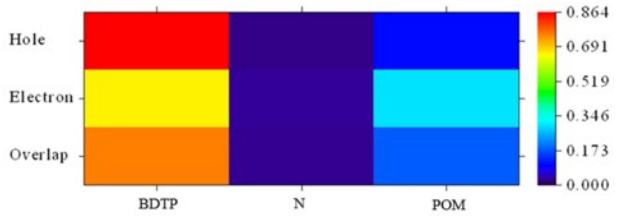

TD/POM

TD : **Hole: 81.06 %** Electron: 4.95 %
N : Hole: 4.34 % Electron: 0.36 %
POM : Hole: 14.60 % **Electron: 94.69 %**

Transferred electrons between fragments:

1 → 2: 0.00291	2 → 1: 0.00215	Net 1 → 2: 0.00076
1 → 3: 0.76753	**3 → 1: 0.00723**	**Net 1 → 3: 0.76031**
2 → 3: 0.04111	3 → 2: 0.00052	Net 2 → 3: 0.04059

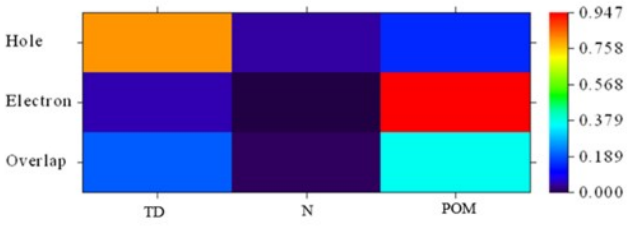

Figure S4. Heat map of the studied designed hybrids (Fragments exhibiting the greatest proportion of hole and electron involvement, as well as the highest rates of electron transfer between fragments are bolded).

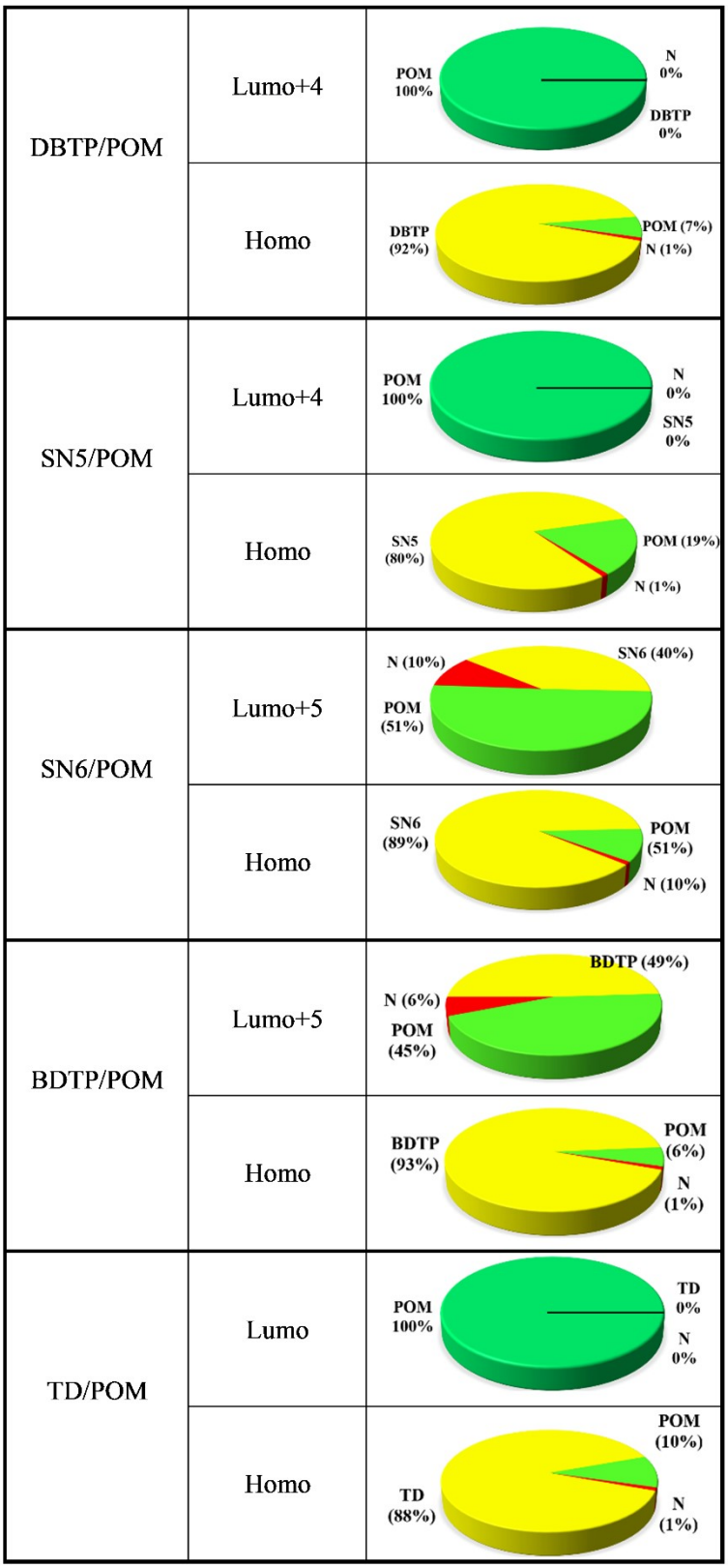

Figure S5. The percentage of each fragment to the molecular orbitals of the studied designed hybrids

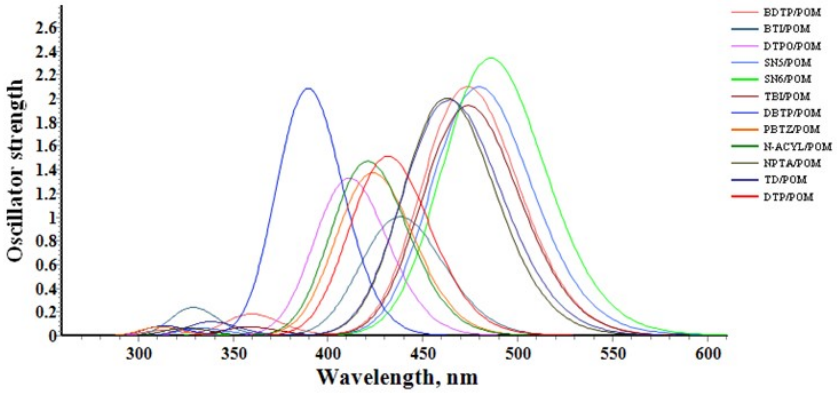

Figure S6. Simulated absorption spectra of the studied designed hybrids

Refrences:

(1) Le Bahers, T.; Adamo, C.; Ciofini, I. A qualitative index of spatial extent in charge-transfer excitations. *J. Chem. Theory Comput.* **2011**, *7* (8), 2498–2506.
(2) Grätzel, M. Recent advances in sensitized mesoscopic solar cells. *Acc. Chem. Res.* **2009**, *42* (11), 1788–1798.
(3) Marinado, T.; Hagberg, D. P.; Hedlund, M.; Edvinsson, T.; Johansson, E. M.; Boschloo, G.; Rensmo, H.; Brinck, T.; Sun, L.; Hagfeldt, A. Rhodanine dyes for dye-sensitized solar cells: spectroscopy, energy levels and photovoltaic performance. *Phys. Chem. Chem. Phys.* **2009**, *11* (1), 133–141, 10.1039/B812154K.
(4) Yan, L.; Jin, M.; Song, P.; Su, Z. Electronic properties of unprecedented bridging organoimido-substituted hexamolybdate: new insights from density functional theory study. *J. Phys. Chem. B* **2010**, *114* (11), 3754–3758.
(5) Zhang, J.; Li, H. -B.; Geng, Y.; Wen, S. -Z.; Zhong, R.-L.; Wu, Y.; Fu, Q.; Su, Z. -M. Modification on C219 by coumarin donor toward efficient sensitizer for dye sensitized solar cells: a theoretical study. *Dyes and Pigm.* **2013**, *99* (1), 127–135.
(6) Koopmans, T. Ordering of wave functions and eigenenergies to the individual electrons of an atom. *Physica* **1933**, *1*, 104–113.
(7) Feng, J.; Jiao, Y.; Ma, W.; Nazeeruddin, M. K.; Grätzel, M.; Meng, S. First principles design of dye molecules with ullazine donor for dye sensitized solar cells. *J. Phys. Chem. C* **2013**, *117* (8), 3772–3778.
(8) Katoh, R.; Furube, A.; Yoshihara, T.; Hara, K.; Fujihashi, G.; Takano, S.; Murata, S.; Arakawa, H.; Tachiya, M. Efficiencies of electron injection from excited N3 dye into nanocrystalline semiconductor (ZrO_2, TiO_2, ZnO, Nb_2O_5, SnO_2, In_2O_3) films. *J. Phys. Chem. B* **2004**, *108* (15), 4818–4822.
(9) Daeneke, T.; Mozer, A. J.; Uemura, Y.; Makuta, S.; Fekete, M.; Tachibana, Y.; Koumura, N.; Bach, U.; Spiccia, L. Dye regeneration kinetics in dye-sensitized solar cells. *J. Am. Chem. Soc.* **2012**, *134* (41), 16925–16928.
(10) Maestre, J. M.; Lopez, X.; Bo, C.; Poblet, J. M.; Casan-Pastor, N. Electronic and magnetic properties of α-Keggin anions: A DFT study of $[XM_{12}O_{40}]^{n-}$, (M = W, Mo; X = Al^{III}, Si^{IV}, P^{V}, Fe^{III}, Co^{II}, Co^{III}) and $[SiM_{11}VO_{40}]^{m-}$ (M = Mo and W). *J. Am. Chem. Soc.* **2001**, *123*, 3749–3758.